

**Microstructure and crystallographic characteristics of  
stenolaemate bryozoans (Phylum Bryozoa, Class  
Stenolaemata)**

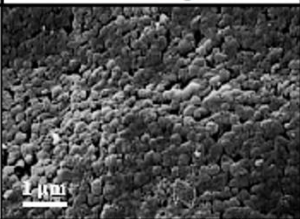
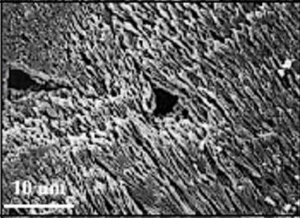
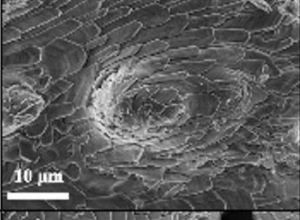
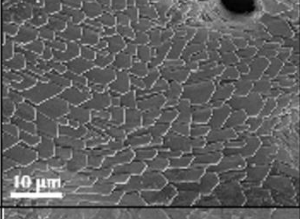
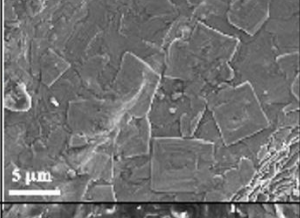
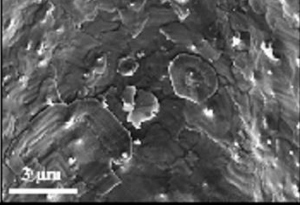
*Christian Grenier<sup>1,2</sup>, Erika Griesshaber<sup>3</sup>, Wolfgang W. Schmahl<sup>3</sup>, Antonio G. Checa<sup>1,2</sup>*

<sup>1</sup>Departamento de Estratigrafía y Paleontología, Universidad de Granada, 18071 Granada, Spain

<sup>2</sup>Instituto Andaluz de Ciencias de la Tierra, CSIC-Universidad de Granada, 18100 Armilla, Spain

<sup>3</sup>Department of Earth and Environmental Sciences, Ludwig-Maximilians Universität, 80333 Munich,  
Germany

**Supplementary Figures S1 to S16**

Fabric	Description	SEM image
Granular	Equidimensional crystallites randomly oriented (Example of <i>Patinella radiata</i> ) (Taylor and Weedon, 2000)	
Planar spherulitic	Fan or strip oriented parallel to wall growth direction (Example of <i>Coronopora truncata</i> ) (Taylor and Weedon, 2000)	
Transversaly fibrous	Long lath-like flattened crystallites, imbricated, growing at acute angles (Example of <i>Cinctipora elegans</i> )	
Foliated	Long lath-like flattened crystallites, imbricated, growing at obtuse angles (Example of <i>Fasciculipora ramosa</i> )	
Rhombic semi-nacre	Rhombio-shaped tablets crystallites growing with screw dislocations (Example of <i>Harnera robusta</i> )	
Hexagonal semi-nacre	Hexagonal-shaped tablets crystallites growing with screw dislocations (Example of <i>Harnera robusta</i> )	

**Figure S1.** Summary table of the six different microstructures described by Taylor and Weedon (2000) in stenolaemate bryozoans.

<b>Species</b>	<b>Provenance</b>	<b>Classification</b>
<i>Fasciculipora ramosa</i> (d'Orbigny, 1842)	36 <sup>th</sup> Soviet Antarctic Expedition Federov Stn 19(3) 393 metres 13/01/1991.	Class Stenolaemata; Order Cyclostomatida.
<i>Cinctipora elegans</i> (Hutton, 1873)	Otago Shelf, New Zealand Ca 80-100 m 1995.	
<i>Hornera robusta</i> (MacGillivray, 1883)	Otago Shelf, New Zealand Ca 82 m Stn Mu 88-28 May, 1988	

**Figure S2.** List of the species analyzed in the present study.

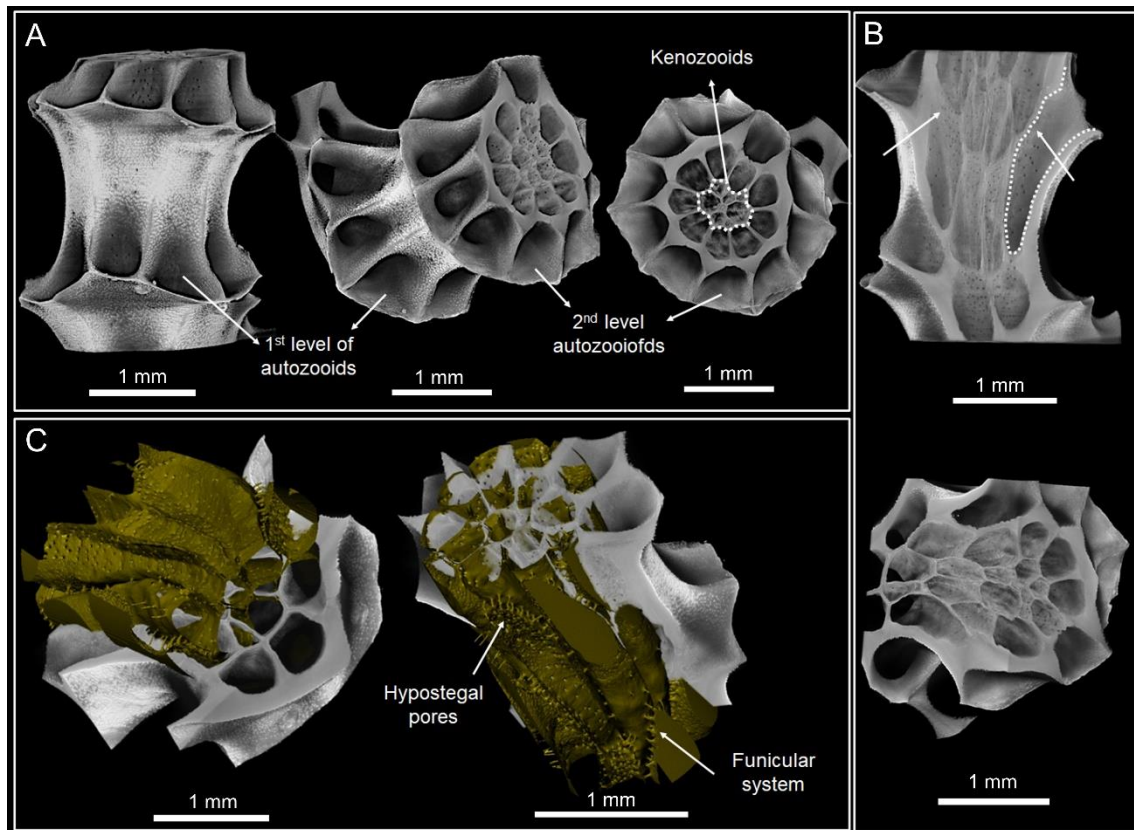


**Figure S3.** Micro CT images from *Cinctipora elegans*. A. From left to right: frontal, oblique and zenithal views of the cylindrical colony fragment analysed. Concentrically disposed 1st and 2nd level autozooids (indicated) can be observed. In the central region, the structural kenozooids are delimited with white dashed lines. B. Longitudinal (top) and oblique (bottom) views of the colony. The conical-tubular shaped zooid chambers (wider at the aperture) are concentrically arranged. They are connected to each other through interzooidal pores, which are more numerous towards the kenozooids. Interzooidal walls (indicated with white arrows) separate two generations of autozooids that remain connected by the hypostegal pores. C. Oblique views of a longitudinal section of the colony. The reconstructed interior volumes of the zooid chambers are interconnected by channels (funicular system). The hypostegal pores, through which budding growth proceeds, are indicated.

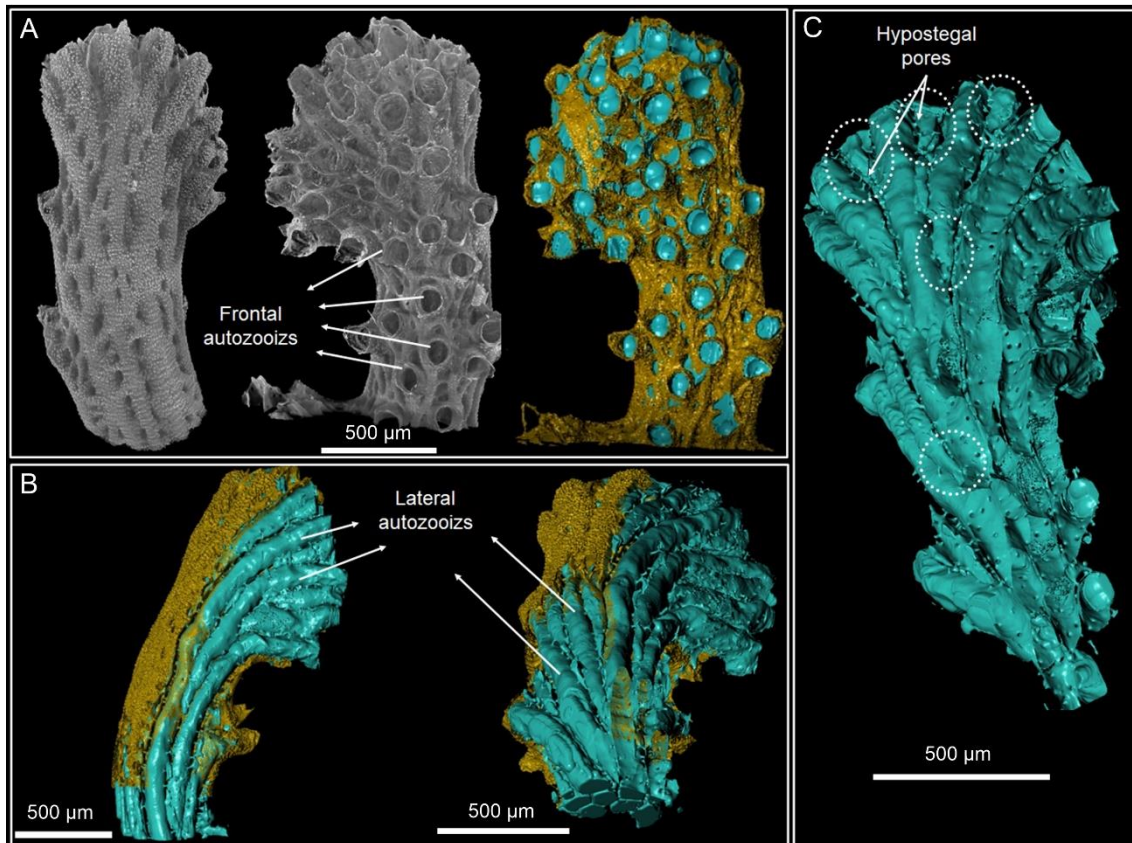


**Figure S4.** Micro CT images of *Hornera robusta*. A. Abfrontal (left) and frontal (center) views of the colony fragment analyzed. The micro-CT reconstruction (right) shows the inner volume of the zooid chambers (cyan) and the skeleton (gold). B. Same reconstruction in lateral (left) and oblique (right) views, with the skeleton partially removed to show the long tubular shape and the disposition of the lateral autozooids (white arrows), projected toward the front. They are connected to each other through the interzooidal pores (funicular system). C. Inner volume reconstruction of a partly sectioned colony in posterior view. New generations of autozooids, connected with to the parental autozooids by hypostegal pores, are indicated (dashed circles).

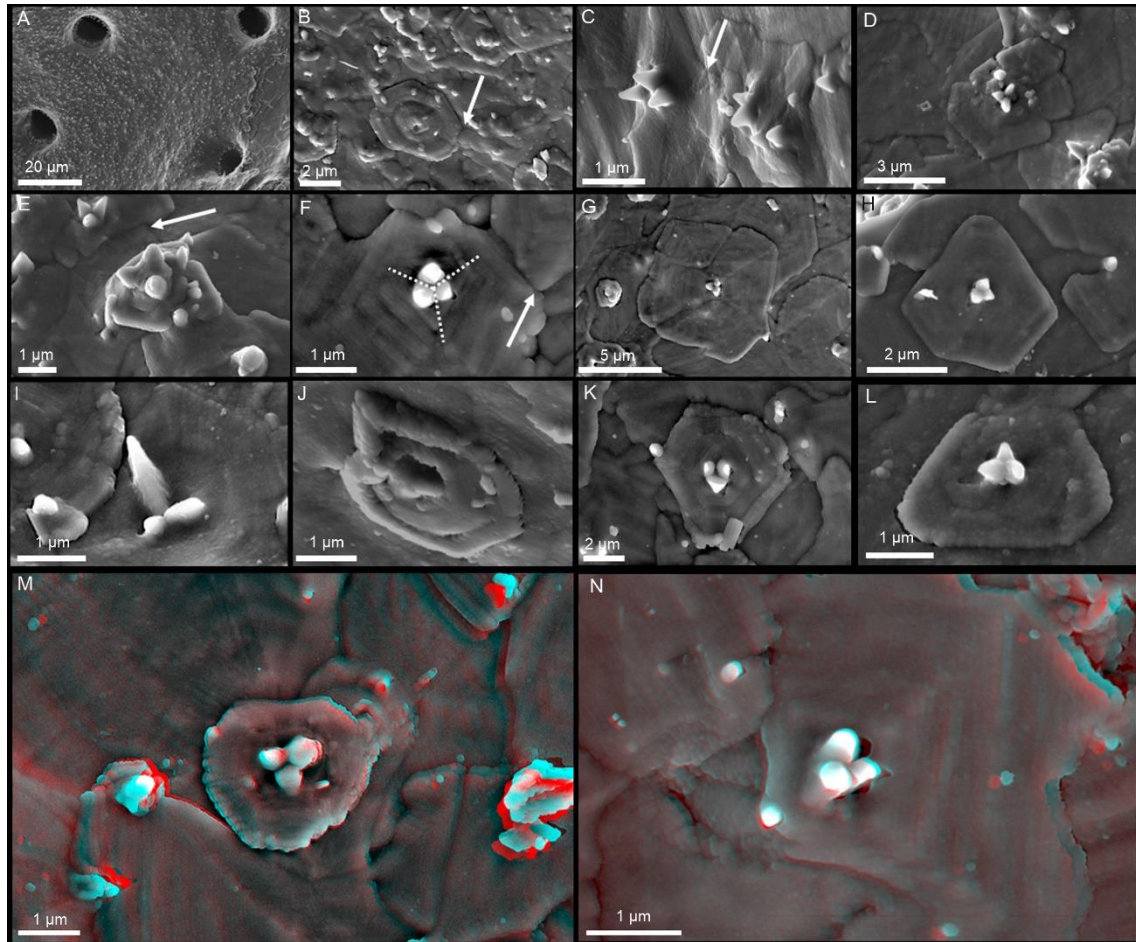


**Figure S5.** Tabular calcite of *Hornera robusta*. All images are from the inner surface of the zooidal chambers, previously cleaned with commercial bleach (5%, 1h). A, B. Overviews of the inner surface. C-L. Close-up views of different examples of tabular calcite. The polygonal tablets that are at the same level cease to grow when their margins collide (arrows in B, C, E and F). New tablets overlap previous ones, except for their spikes (E, H, K). Polygonal outlines vary from triangular to hexagonal. Growth lines and nanoroughness on the surfaces of the tablets are clearly discernible. The triple-spiked outgrowths are from 100 nm to 300 nm in height, exceptionally up to 1 micron (e.g., I). The three spikes are oriented at  $120^\circ$  from each other (e.g., F). M and N are anaglyphs. To appreciate the 3D effect, red-cyan glasses have to be used.

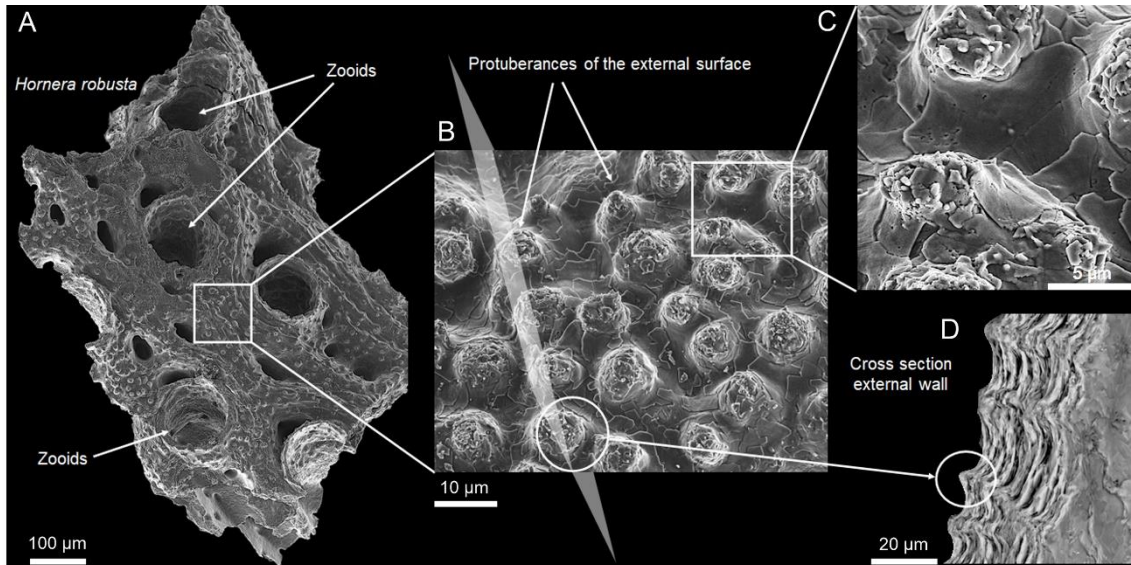


**Figure S6.** Topography of the outer surface of *Hornera robusta*. A. Colony fragment. B. Closer view of the outer surface studded by numerous protuberances. The white semi-transparent area represents the cross-sectional plane of the fragment shown in D. C. Detail of the outer surface showing the microstructure, constituted by the same polygonal tablets as found in the zooidal chambers interior. The calcite tablets partly imbricate and appear heavily distorted due to surface irregularities. D. External wall section where the protuberances have been cut transversely, showing the multi-layered undulated wall where the crests of the waves coincide with the protuberances.

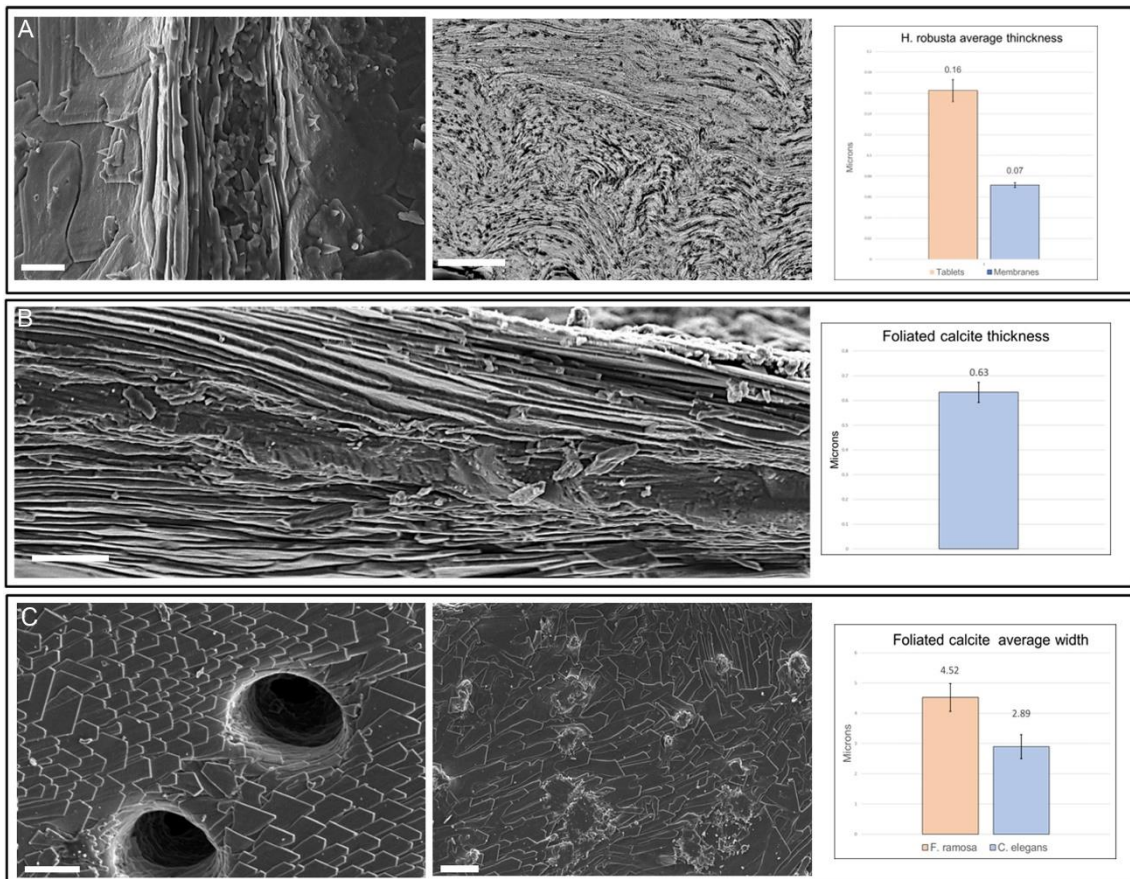


**Figure S7.** Tabular and foliated calcite measurements performed on SEM images. A. Average thickness of the tablets of *H. robusta* at an inner wall section and of the intervening membranes at a cross section of the external wall. B. Average thickness of the laths of *F. ramosa* at an inner wall section. C. Average width of the laths at the inner surface of *F. ramosa* (left) and *C. elegans* (right). Vertical segments in the bars indicate the standard error, calculated from the standard deviation.

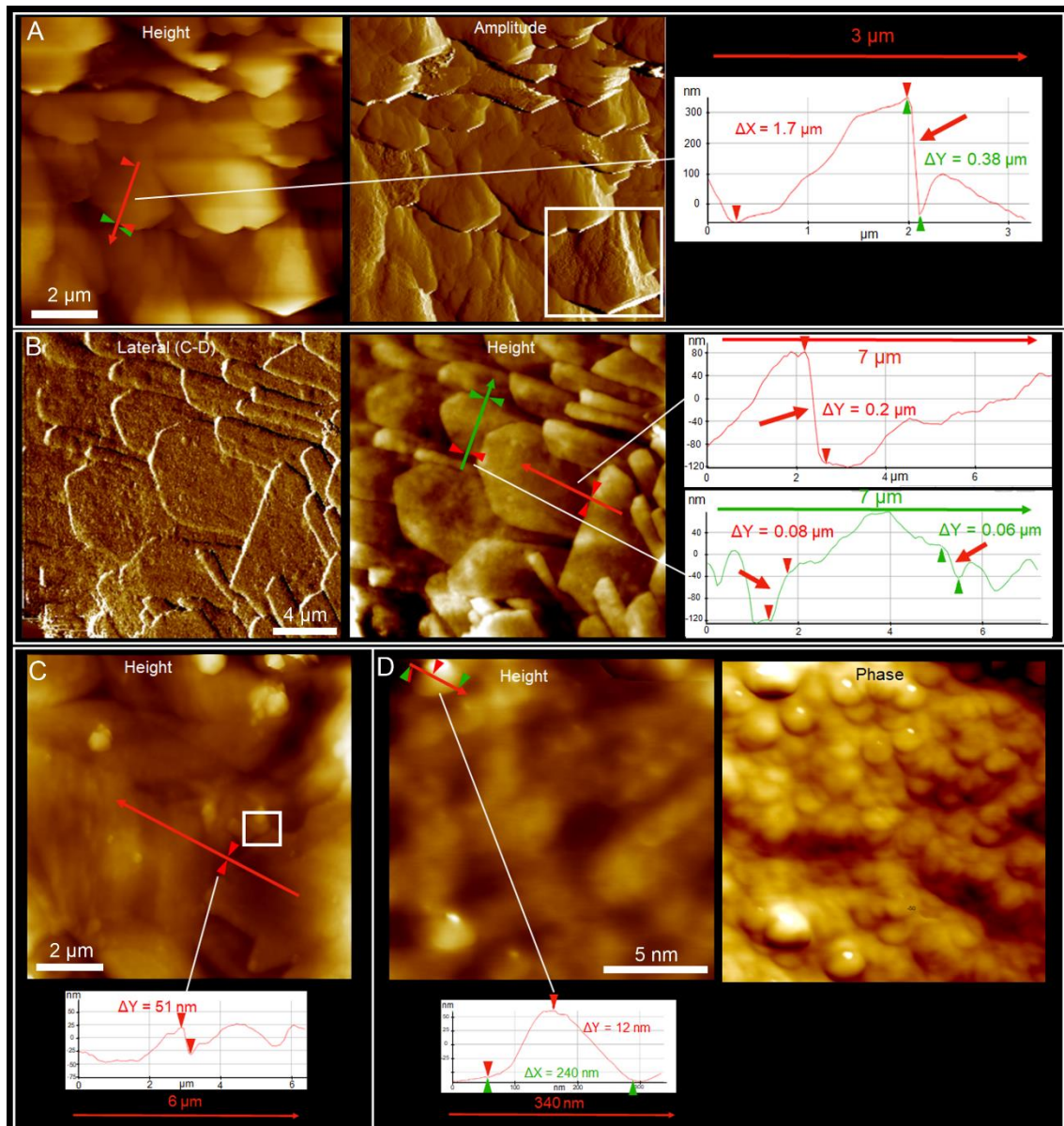


**Figure S8.** AFM analysis of the foliated and tabular calcite of *Fasciculipora ramosa* (A and B) and *Hornera robusta* (C and D). A. Height and amplitude images of a set of calcite laths. They display characteristic arrowhead endings and are partly imbricated. The irregular surfaces of laths are evident in the amplitude image (e.g. framed lath). The profile graph of the transect marked in the height image shows a smooth highly sloped surface at the tip of the lath (red arrow), with an unevenness of  $0.38 \mu\text{m}$ . B. PinPoint mode of lateral strength and height images from another region. The profiles of the transects delineated in the height image show that the lateral and terminal facets (red arrows) of the laths are highly inclined. C. Height image of calcite tablets, where the polygonal contours and the growth lines are visible. The profile graph shows the high inclination of the lateral slope of a tablet. D. Height and phase images of the area framed in C. The nanoprotrusions of the tablet's surface can be appreciated. The profile graph of a selected nanoprotrusion (red transect in the height image) indicates a height of  $12 \text{ nm}$  and a length of  $240 \text{ nm}$ .

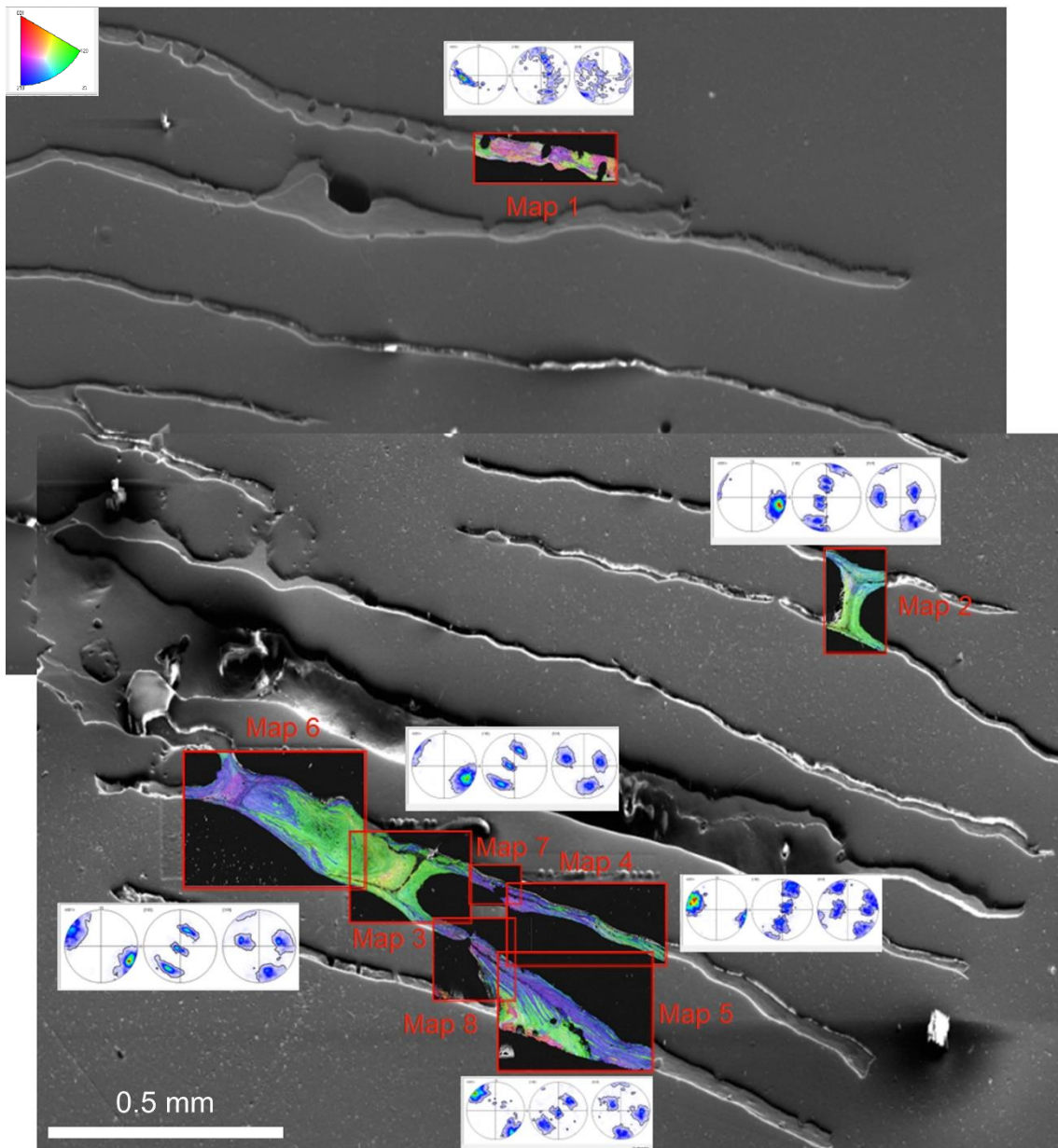


**Figure S9.** General view of the eight EBSD measurements performed on different regions of a *Fasciculipora ramosa* polished sample. EBSD maps with their corresponding pole figures are provided. They indicate a sheet texture in all cases.

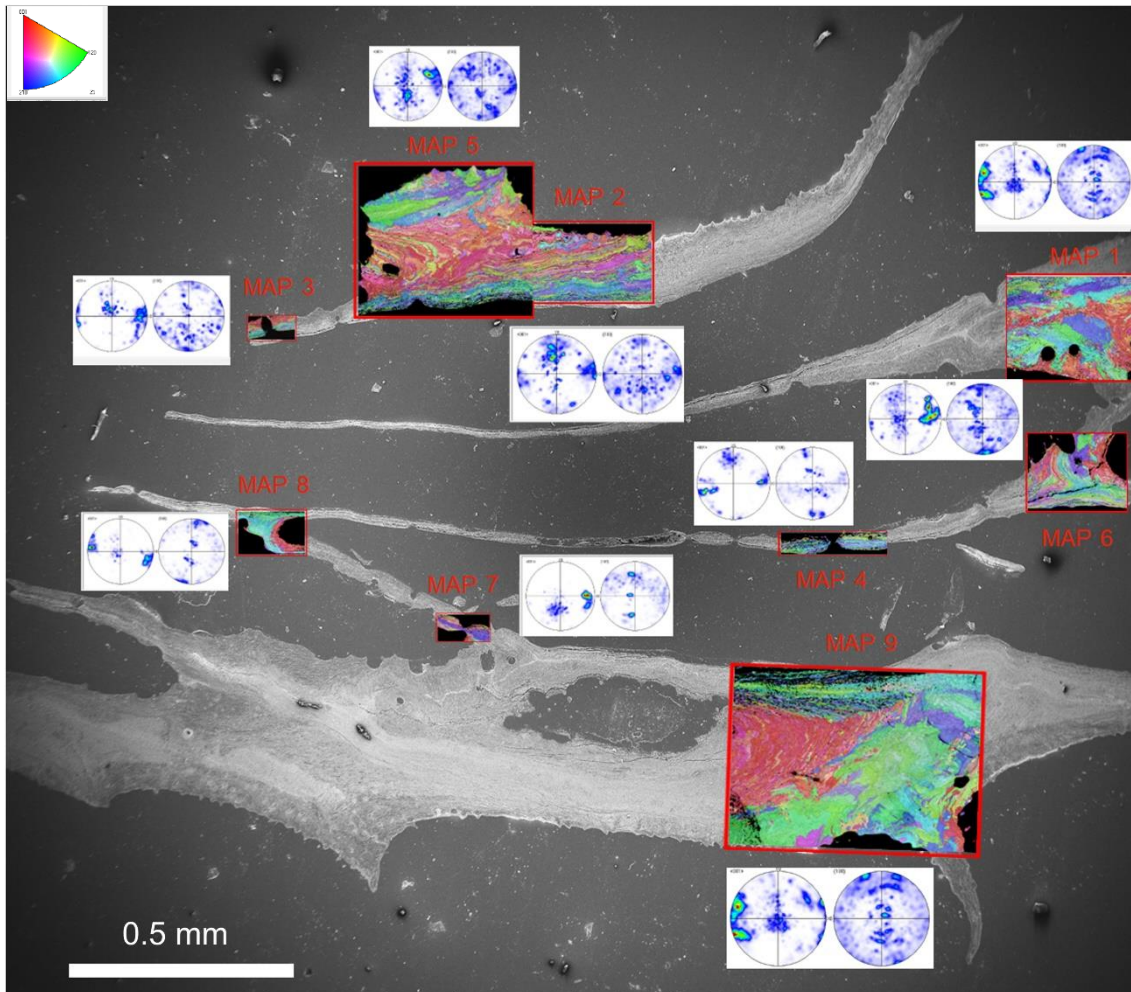


**Figure S10.** General view of the nine EBSD measurements performed on different regions of a *Cinctipora elegans* polished sample. EBSD maps and their corresponding pole figures are provided. They indicate a clear (e.g. maps 4, 7 and 8) or diffuse (1, 2, 3, 5, 6 and 9) sheet texture.

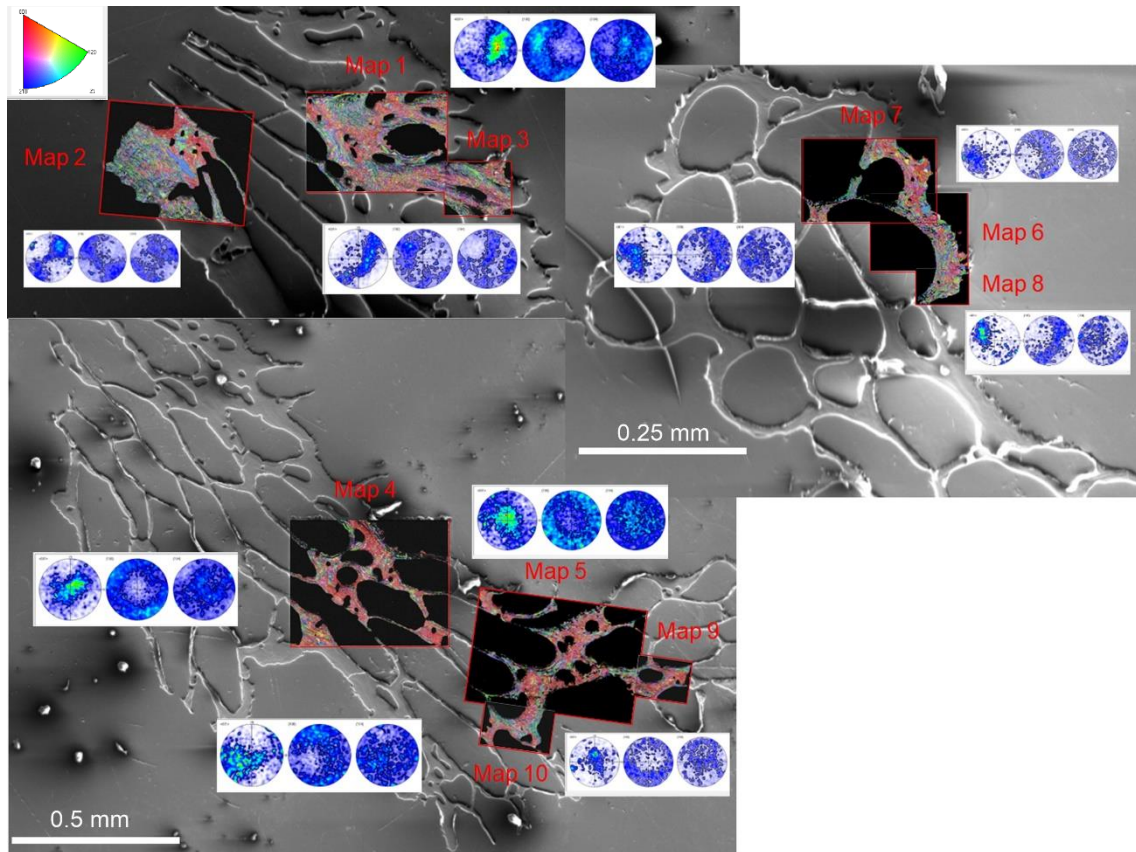


**Figure S11.** General view of the ten EBSD measurements performed on different regions of a *Hornera robusta* polished sample. EBSD maps and their corresponding pole figures are provided. Pole figures indicate an axial texture in all cases.

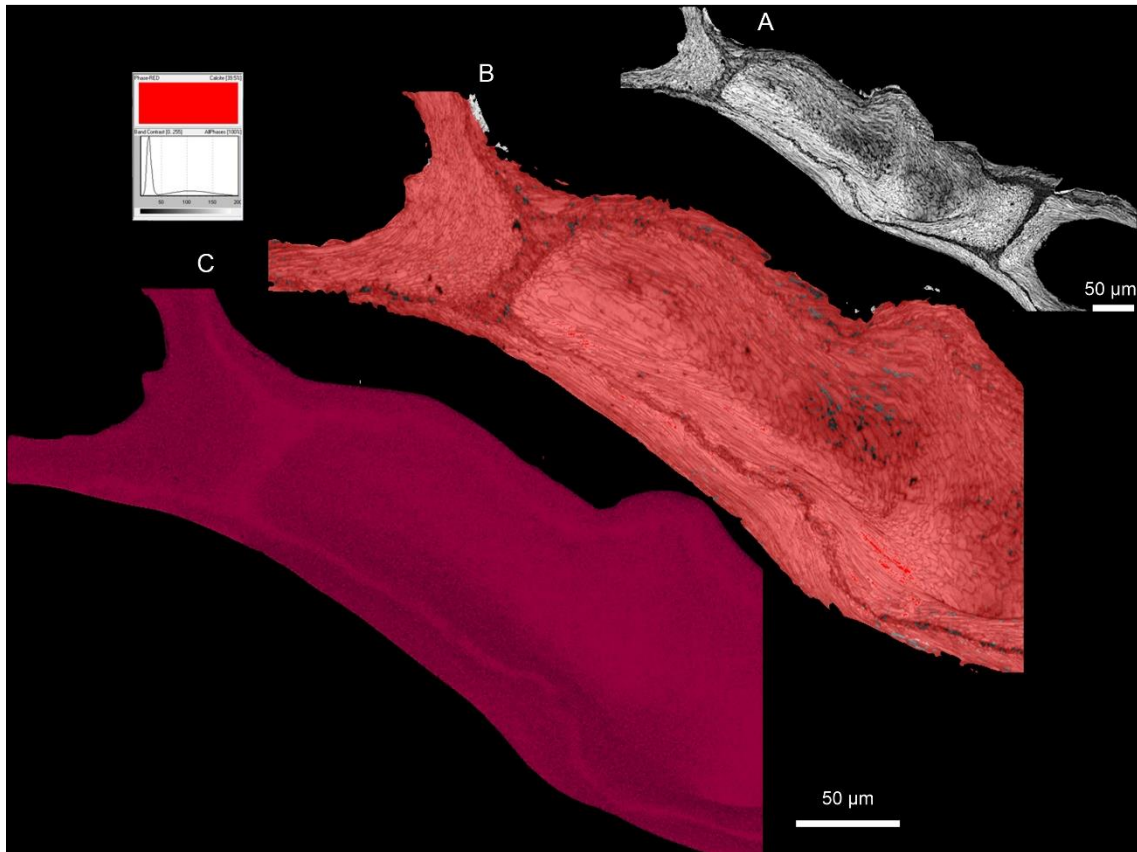


**Figure S12.** EBSD and EDX analysis of the foliated calcite of *Fasciculipora ramosa*. B. EBSD phase map of the area in A. The red color indicates that the entire sample is made of calcite. The color key for the phase is provided. C. EDX map of Mg, showing zonation. The signal is stronger in the granular layer.

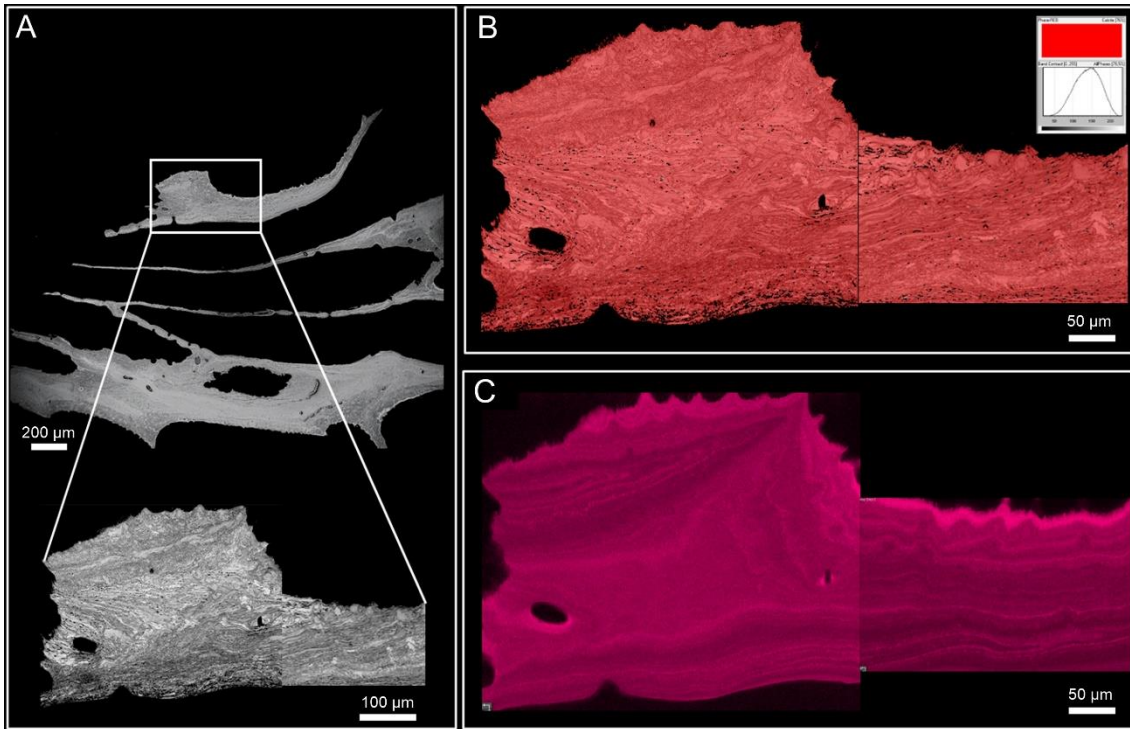


**Figure S13.** EBSD and EDX analysis of the foliated calcite of *Cinctipora elegans*. A. SEM image of a polished colony fragment. The framed region is a section of the external wall at a low angle, shown as the corresponding EBSD band contrast maps. B. EBSD phase map of the area framed in A. The red color indicates that the entire sample is made of calcite. The color key for the phase is provided. C. EDX map of Mg, showing zonation related to particular growth increments, being more intense at the outer surface.

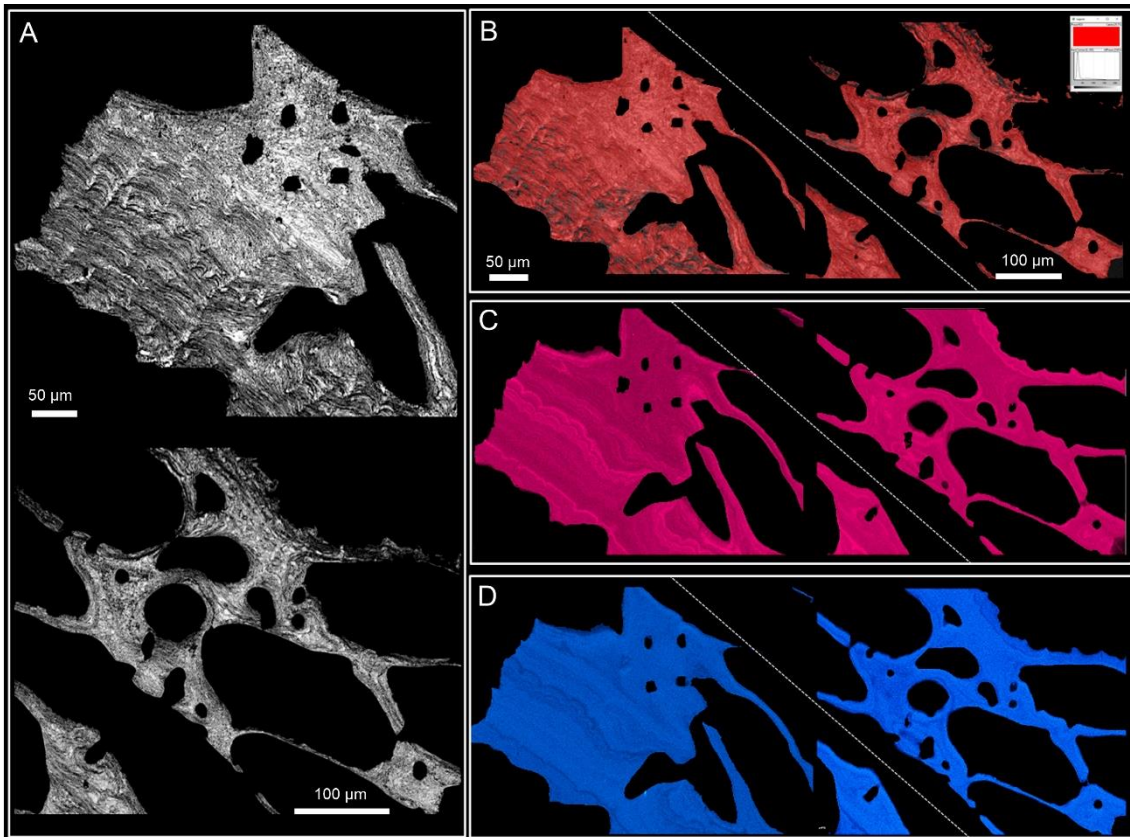


**Figure S14.** EBSD and EDX analysis of the tabular calcite of *Hornera robusta*. A. EBSD band contrast maps in grey-scale from two different areas: a cross-section of the external wall (top) and a section of the colony wall at a low angle (bottom). B. EBSD phase map of both regions. The red color indicates that both samples are made of calcite. The color key for the phase is provided. C and D. Mg (C) and S (D) EDX maps of both regions, showing marked zonations related to growth increments.

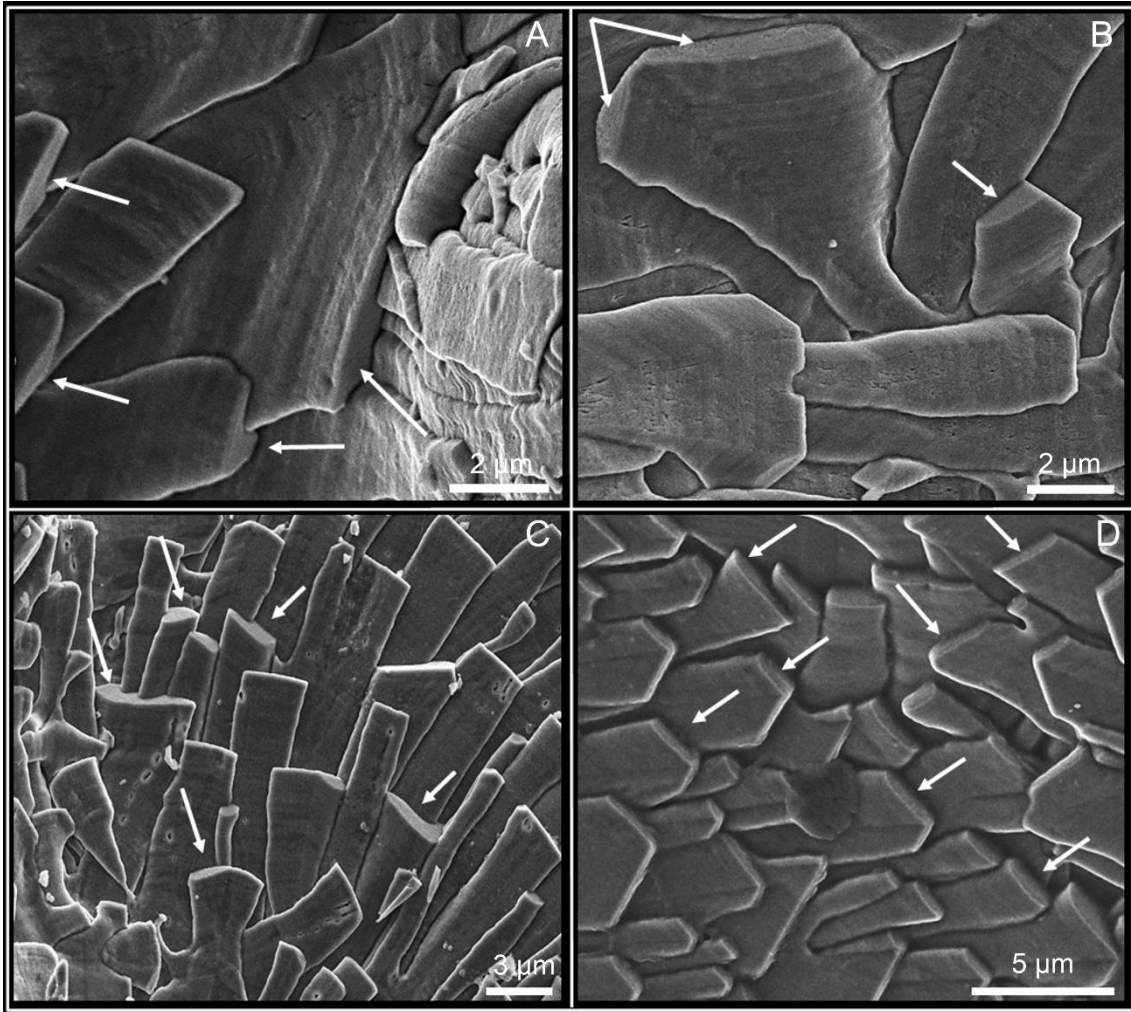


**Figure S15.** Views of the foliated calcite of *C. elegans* (A-C) and *F. ramosa* (D). The main surfaces of the laths are rough, with visible growth lines, whereas the highly inclined terminal surfaces are smooth (arrows).

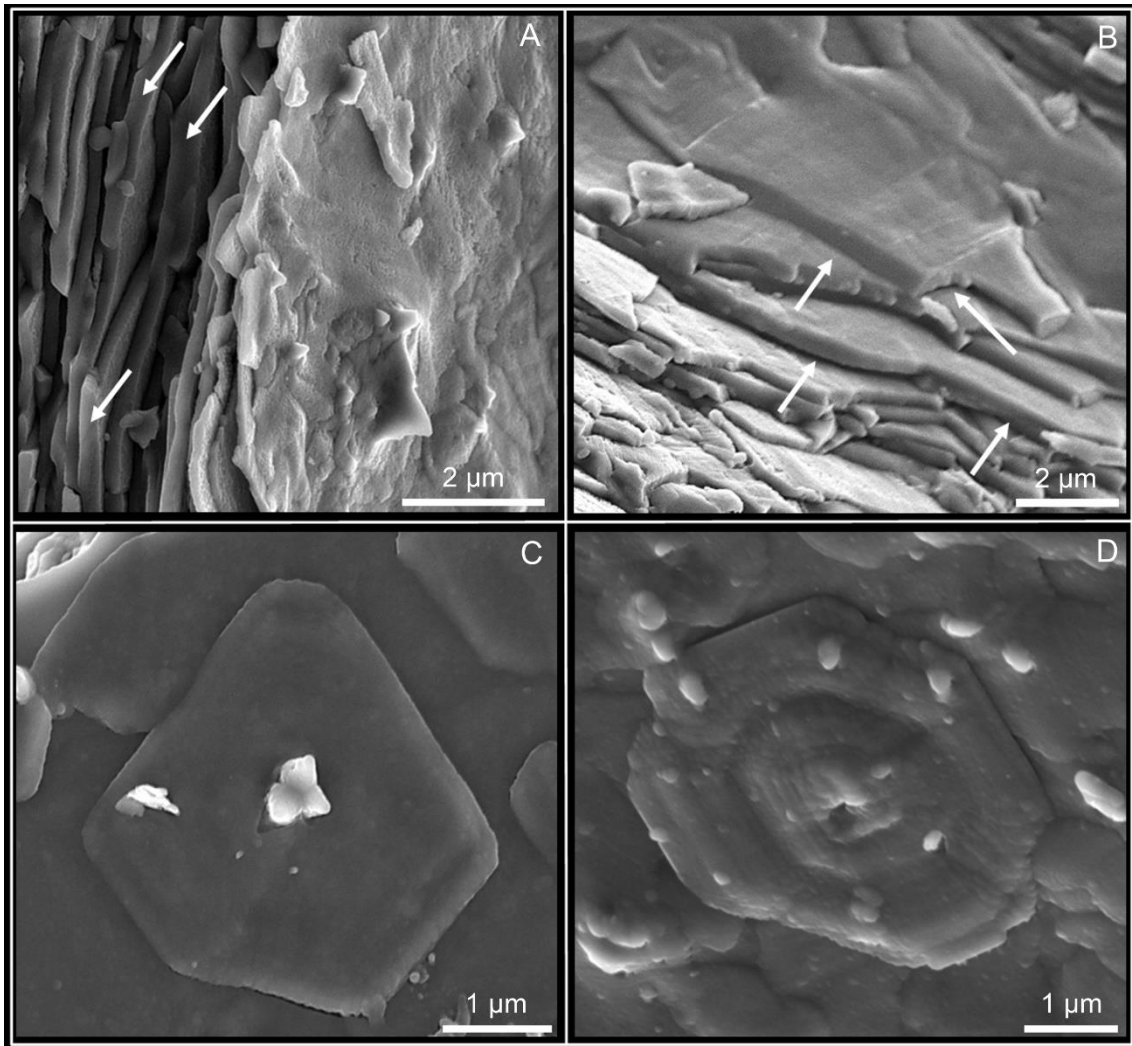


**Figure S16.** Close up views of calcite tablets of *H. robusta*. A, B. Lateral views, showing the highly inclined lateral surfaces. They are smooth and straight (white arrows). C, D. Top views of the rough main surfaces of the tablets, with visible growth lines.